

Sonar-based Chain Following using an Autonomous Underwater Vehicle

Natàlia Hurtós¹, Narcís Palomeras¹, Arnau Carrera¹, Marc Carreras¹, Charalampos P. Bechlioulis², George C. Karas², Shahab Hesmati-alamdar², Kostas Kyriakopoulos²

Abstract—Tracking an underwater chain using an autonomous vehicle can be a first step towards more efficient solutions for cleaning and inspecting mooring chains. We propose to use a forward looking sonar as a primary perception sensor to enable the vehicle operation in limited visibility conditions and overcome the turbidity arisen during marine growth removal. Despite its advantages, working with acoustic imagery raises additional challenges to the involved image processing and control methodologies. In this paper we present a robust framework to perform chain following, combining perception, planning and control disciplines. We first introduce a detection system that exploits the sonar’s high frame rate and applies local pattern matching to handle the complexity of detecting link chains in acoustic images. Then, a planning system deals with the dispersed detections and determines the link waypoints that the vehicle should reach. Finally, the vehicle is guided through these waypoints using a high level controller that has been tailored to simultaneously traverse the chain and keep track of upcoming links. Experiments on real data demonstrate the capability of autonomously follow a chain with sufficient accuracy to perform subsequent cleaning or inspection tasks.

I. INTRODUCTION

Persistent autonomy is a subject of increasing efforts in the marine robotics community. The present work is within the context of PANDORA European FP7 project [1], which aims to increase the range and complexity of underwater tasks that can be automated while reducing the need for operator supervision. To this end, one of the three core tasks of PANDORA project is to work towards a cost and time efficient solution for the cleaning and inspection of mooring chains using an autonomous underwater vehicle (AUV).

Chain moorings on floating structures such as floating production, storage and offshore (FPSO) vessels are exposed to severe environmental and structural conditions. In order to avoid potential damage, chain status is monitored through periodic and exhaustive inspections. Traditional methods, which involve recovering the chain on deck or ashore, are being replaced by in situ in-water inspections using remotely operated vehicles (ROVs) equipped with optical callipers [2] [3]. However, most available solutions require prior removal

This work was supported by the EU funded project PANDORA: Persistent Autonomy through learnNing, aDaptation, Observation and ReplAnning”, FP7-288273, and the Spanish Project ANDREA/RAIMON (Ref CTM2011-29691-C02-02) funded by the Ministry of Science and Innovation.

¹Computer Vision and Robotics Group (VI-COROB), University de Girona, 17071 Girona, Spain {nhurtos,npalomera,acarrera,marcc}@eia.udg.edu

²School of Mechanical Engineering, National Technical University of Athens, Athens 15780, Greece {chmpechl,karrasg,shahab, kkyria}@mail.ntua.gr.

of the marine biofouling so that the chain can be properly examined. Cleaning solutions range from manual brushing with divers, which is potentially hazardous and has an inherent depth limit, to high-pressure water systems deployed with ROVs [4]. The time spent to clean strongly depends on the selected option, but in general is a tedious and slow task since the optical visibility drops drastically as the removed marine growth floats in the water. Indeed, considering the cost of ROV vessels, chain cleaning can be a significant fraction of the cost of a chain inspection program [4].

To avoid the presence of troublesome ROV cables and reduce the cost of the deploying vessel, the PANDORA project aims to demonstrate the feasibility of using an AUV equipped with a water jet to conduct chain cleaning and inspection tasks. Our proposal is to use an AUV with a high resolution imaging sonar [5], which delivers acoustic images at near-video frame rate, in order to autonomously navigate along the chain and detect each of the links. In this way the cleaning process can be carried out regardless of the visibility conditions and the suspended marine fouling, thus speeding up the overall operation. Moreover, by producing an enhanced composition of the images gathered along the chain trajectory, the same methodology provides the means to perform an initial visual inspection, from which it is possible to identify some major issues or locate problematic parts that need further inspection.

Despite these advantages, the use of such a system arises several challenges that must be addressed. First, the automatic detection of the chain links in forward-looking sonar (FLS) images becomes a complex problem due to the inherent sonar characteristics: noise, low resolution, moving shadows and intensity variations due to different vantage points. Besides, the control of the AUV must be adapted to take into account the imaging geometry of the sonar. The vehicle location at a given instant differs from the point that is being inspected, which is located few meters ahead depending on the sonar’s range configuration. Thus, to successfully follow the chain, the detection and control schemes must be tightly coupled and be able to react in real-time. Otherwise, chain links can easily drop off the sonar’s narrow field of view resulting in the vehicle losing track of the chain.

This paper deals with the problem of autonomously following an underwater chain as a first step towards performing chain cleaning and inspection with an AUV. An overview of the proposed framework is explained in Section II. Section III describes the detection algorithm developed to robustly detect chain links on sonar imagery. Section IV covers the

generation of position waypoints from the link detections. Section V describes the control system of the AUV, adapted to concurrently navigate over the estimated link waypoints and keep the proper vehicle orientation to follow the upcoming links. Experiments and results are reported in Section VI, showing the performance of the chain following framework on real experiments with a chain mock-up. Finally, Section VII concludes the paper and points out future work.

II. SYSTEM OVERVIEW

Figure 1 outlines the developed chain following framework. Our mission scenario consists in an AUV that is deployed in the vicinity of a mooring chain end. The present methodology considers a chain lying approximately on a plane, either horizontal or vertical. Note though, that the approach could be extended to other configurations with the aid of a pan-and-tilt unit in order to set the imaging sonar to the appropriate grazing angle.

The stream of sonar images is processed by a link detection module that identifies the presence of a chain link within the sonar's field of view and delivers its position with respect to the sonar's origin. Notice that our aim is to detect each of the links as accurately as possible as the system is intended to clean them appropriately.

By taking into account the sonar position in the vehicle and the vehicle location in the world coordinate frame, link detections provided by the previous module are referenced with respect to the world coordinate frame. The different detections are grouped and associated to the corresponding chain links by a second module, named waypoint planner. This module maintains a list of all detected links and generates an ordered sequence of world waypoints that have to be visited in order to correctly follow the chain.

Finally, a third module implements a combined control system which guides the vehicle towards each sequence's waypoint while keeping the orientation to the last detected link. In this way, the vehicle visits the links that have already been identified while new ones are simultaneously detected and added to the list. This process is executed until the vehicle has reached the position of the last visible link and no link remains unvisited thus having completed the chain following procedure.

The details of the cleaning system, by means of a water jet integrated on the AUV, fall beyond the scope of the presented framework. However, a new low level controller that will be integrated into the described control module is already being developed [6] to be able to cope with the perturbations originated by the water jet.

III. DETECTION OF CHAIN LINKS ON FLS IMAGERY

Although the resolution of new FLS devices is progressively increasing, the inherent characteristics of the acoustic images pose a challenge to the object detection techniques that are typically used on optical images. For instance, the low degree of repeatability when extracting point features in sonar images [7] turns into unfeasible detection approaches that involve matching features against a visual vocabulary of

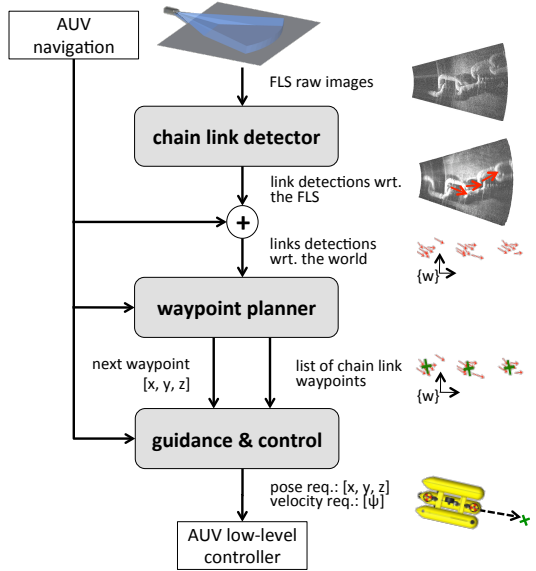


Fig. 1: Diagram illustrating the different steps of the chain following framework.

an object. A common practice in sonar object recognition is to take advantage of shadow cues. Given that chain links are not isolated objects but interlaced elements, it is difficult to exploit the use of shadows as they cannot be distinctly identified. Likewise, gradient-based or edge-based techniques become unreliable as depending on the link's position there is a wide range of different outcomes in image intensities. There are many possible intensity transitions (from link to background, link to shadow, link to link, shadow to background) together with possible sonar artefacts (e.g. cross-talk or strong reflections) that can contribute to fragment and clutter an edge map, thus complicating the task of identifying the link's contour.

The proposed detection method relies mainly on the intensities backscattered by the link itself, which are most of the times under partial occlusions due to the imaging viewpoint or actual objects occluding parts of the chain link, such as other links or marine growth. We have approached the problem as a pattern matching using normalized cross-correlation of local templates, which allows us to detect portions of the link while others are not visible. Those detections are then robustly clustered and related according to their known dimensions and spatial location to finally identify the presence of a link and provide an estimation of its center and orientation. Fig. 2 summarizes the link detection process, consisting of the following steps:

- **Image enhancement:** Instead of performing the detection on a raw frame, the system takes advantage of the sonar's high frame rate and registers a small number of n consecutive frames to produce an intermediate image of increased signal to noise ratio. The registration between frames is performed using Fourier-based techniques [8] and the resulting image is formed by averaging the intensities at each point thus reducing the noise and the incidence of

spurious artefacts present in the individual frames.

- **Pattern matching:** The image generated in the previous step is the basis for performing cross-correlation with local templates, each one rotated in few different orientations. These templates have been previously defined according to the morphology of the particular chain that has to be followed (e.g, for a studless chain a good template set would be composed of the four link corners and the straight side). Although many links might be present in one image, and therefore several areas can reflect a high correlation response for a given template, only the strongest location for each template is kept.
- **Clustering of detections:** To increase robustness and discard outliers, local detections are accumulated along several images, according to the displacements identified by registration. These detections are clustered by template type, ensuring that a minimum number of the same type are located within a neighbourhood in order to consider a detection as valid.
- **Link identification:** Clustered detections must be associated into groups belonging to the same link. To that end we make use of a heuristic that explores a sequence of possibilities according to the cluster's spatial location and known link dimensions. Due to link interlacing, alternate links have different inclinations with respect the main chain axis, making link elements of one side easier to be seen at a given image. Therefore the heuristic sweeps the image for the combination or sub-combination of link elements of the same side (i.e [lower-left corner/straight segment/upper-left corner] or [lower-right corner/straight segment/upper-right corner]).
- **Orientation estimation:** Once the different links have been identified, orthogonal regression is used to fit a line through the detections composing the different groups of a link. The orientation of the fitted line serves as an estimate of the link's orientation.
- **Center estimation:** Finally, using the estimated angle the location of the link's center can be estimated by projecting the known link dimensions from each detection point, assuming a 2D projection.

IV. WAY-POINT PLANNER

As the vehicle moves, the same link might be observed and detected multiple times through the module presented in previous section. However, these estimations will vary around the actual chain link center due to mainly two reasons. On the one hand, the locations found in the template matching step can slightly differ from one observation to the other as the image's intensities fluctuate due to small viewpoint changes. Therefore, the detected location of a link's part may be slightly different and so may be the final center estimation. On the other hand, since the detections are referenced in a world map by using the position of the vehicle, the accumulated navigation drift between two detections may diverge their positions. In view of that, we developed a module that: a) classifies the different estimations of the centers into clusters that belong to the same chain link and

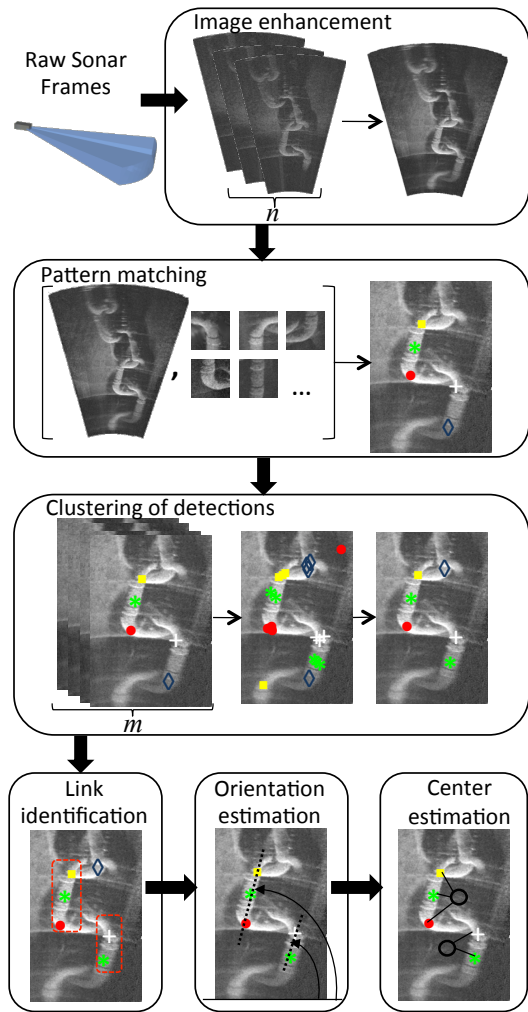


Fig. 2: Diagram of the link detection steps.

b) sorts the clusters in order to request to the vehicle the next way point that needs to be reached to follow the chain.

Therefore, the planner module will maintain a list of ordered way points referring to the centers of the detected chain links. The output of this module at a given instant is the next waypoint that needs to be reached. Initially, the requested waypoint is the first of the list. When the vehicle reaches the desired location (considering a surrounding tolerance area) the requested waypoint will then change to the next one.

The computation of the way points is performed in three main steps. First, an n -th order polynomial curve $y = p_n(x) = \sum_{i=0}^n a_{n-i}x^{n-i}$ is fitted on the sonar detection data (x_i, y_i) , $i = 1, \dots, N$, where N is the total number of link center estimations provided by the detection module up to a given instant - see Fig. 3a-3b. The polynomial fitting is performed using the least squares method. Notice that the degree n of the polynomial is a parameter that must be set according to the smoothness of the chain shape, the smoother the shape is, the lower the value of n should be selected. In general, it will be small ($3\text{-}4^\circ$) as we do not expect the shape of the chain to have abrupt direction changes.

In a second step, the sonar detection data is projected onto the fitted curve, thus resulting in (x_i^{proj}, y_i^{proj}) , $i = 1, \dots, N$ - see Fig. 3c. The projection of each point (x_i, y_i) can be easily performed by finding the closest point to the polynomial through the solution of the following system of two equations:

$$\begin{cases} p_n(x_i^{proj}) &= y_i^{proj} \\ (x_i - x_i^{proj}) + (y_i - y_i^{proj}) \frac{dp_n(x)}{dx} \Big|_{x=x_i^{proj}} &= 0. \end{cases}$$

The first equation dictates that (x_i^{proj}, y_i^{proj}) belongs to the fitted polynomial $p_n(x)$ whereas the second one imposes the fact that the vector $[x_i - x_i^{proj}, y_i - y_i^{proj}]$ is normal to the tangent of the polynomial $p_n(x)$ at the point x_i^{proj} .

Then, the projected data are sorted in increasing order of x values, obtaining $(\bar{x}_i^{proj}, \bar{y}_i^{proj})$, $i = 1, \dots, N$. By computing the distances between two consecutive projected points $\delta_i = \sqrt{(\bar{x}_{i+1}^{proj} - \bar{x}_i^{proj})^2 + (\bar{y}_{i+1}^{proj} - \bar{y}_i^{proj})^2}$, $i = 1, \dots, N-1$ we find those $j \in N_j \subset \{1, \dots, N-1\}$ for which $\delta_j > \bar{\delta}$, where $\bar{\delta}$ denotes half the length of a chain link. If $\delta_j > \bar{\delta}$, points $(\bar{x}_j^{proj}, \bar{y}_j^{proj})$ and $(\bar{x}_{j+1}^{proj}, \bar{y}_{j+1}^{proj})$ are classified in different classes belonging to different chain links - see Fig. 3d. Note that $N_j + 1$ defines the number of total different detected chain links. Finally, we estimate the center of the detected chain links by computing the centroid of each of the projected data classes.

The estimates of the sonar detection algorithm will be updated as the AUV moves towards the desired way points; hence the described planning scheme is re-computed until there are no further updates.

V. CONTROL SCHEME

The control module is responsible to guide the vehicle to the world waypoints dictated by the planner. However, when the vehicle is over a waypoint, the sonar is inspecting an area located several meters ahead of the current vehicle position (depending on the configured range parameters). In order to perform a seamless chain following we need to ensure that the chain is kept within the field of view of the sonar at all times, regardless of the vehicle position. To that end, our approach consists in a dual high level controller: on one side, a xyz position controller moves the vehicle to the desired waypoint. On the other, a yaw velocity controller has the purpose of keeping the farther perceivable link waypoint in the middle of the sonar's field of view. The world coordinates of the link to be centered are transformed with respect to the mid point of the sonar's field of view. In this way, the error that must be compensated in order to keep the link in the middle of the image corresponds to the y coordinate of the obtained waypoint. By feeding this error to a proportional controller we obtain the velocity setpoint that will correct the yaw rate according to the link's distance to the center. With this strategy we guarantee that the vehicle always points to the farther detected link within the field of view thus

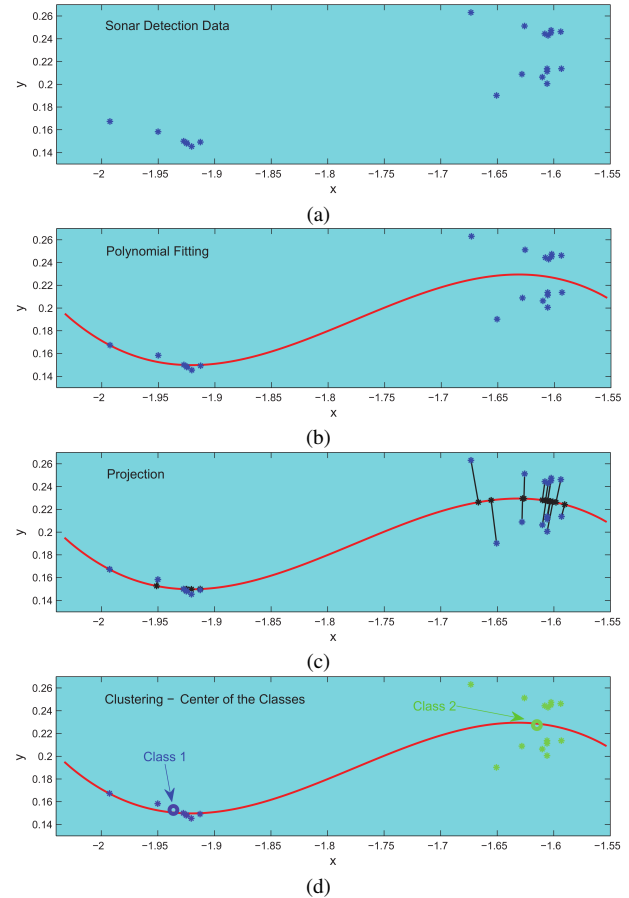


Fig. 3: Phases of the waypoint planner computations. Blue stars: estimates from the sonar detection algorithm. Red solid line: polynomial that fits the sonar data. Black stars: projected points onto the polynomial. The two detected waypoints and their centers are depicted by stars and a circle of the same color in (d).

increasing the possibilities of detecting successive new ones as it moves from waypoint to waypoint.

A special situation occurs if the vehicle reaches a waypoint and there are no links inside the sonar's field of view. This circumstance can take place when: a) the vehicle is arriving to the end of the chain and the links remaining to be visited are already too close to be inside the field of view or b) the chain presents a significant deviation in its trajectory and the links drop off the field of view before being robustly detected thus losing the track of successive links. In those cases the vehicle stops and rotates 45° left and right in order to look around for new links, which, in case of being found are added to the planner list. The execution follows until the vehicle has reached the last waypoint in the list.

VI. EXPERIMENTS AND RESULTS

The validation of the proposed approach has been conducted in the water tank at *Centre d'Investigació en Robòtica Submarina* (CIRS) of the University of Girona using the Girona 500 AUV [9]. The vehicle is equipped with a complete navigation suite including a doppler velocity log, an

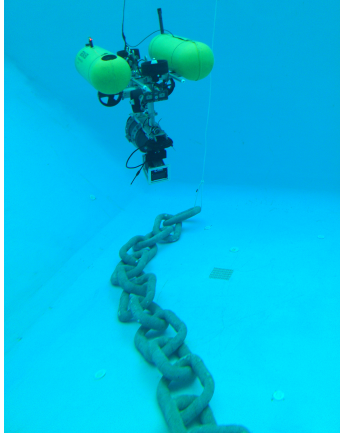


Fig. 4: Experimental setup at the University of Girona's water tank: Girona 500 AUV equipped with the ARIS FLS and a chain segment deployed horizontally at the bottom.

attitude and heading reference system, and a depth sensor. For the purpose of this experiment a SoundMetrics ARIS FLS [5] was installed in the payload area. The ARIS FLS delivers high-resolution acoustic imagery, providing an angular resolution of 0.3° at the expense of having a narrow field of view (30°). The sonar was mounted on a pan and tilt unit and the tilt angle was fixed throughout the experiments to 15 degrees which is a suitable grazing angle for gathering images on the horizontal plane. A replica of a mooring chain, consisting of 13 studless links and measuring approximately 7 meters, was deployed at the bottom of the tank. Fig 4 shows a picture of the setup.

The sonar window was set to 2.5 meters, extending from 1 to 3.5 meters ahead of the vehicle. Such a short ranges were established with the aim of having a better image resolution and avoid, at the same time, reflections from the tank walls. According to the configured range samples, the acquired images (350x497 pixels) have a range resolution of 0.5 cm. The acquisition rate was set to 8 frames per second. At this frame rate, the detector module can generate an enhanced image each 3 frames and accumulate the individual template detections over 4 images thus keeping the processing in real-time and delivering link detections at 0.6 Hz.

To start the experiment the vehicle was teleoperated near one of the chain ends and was left in a position where some chain links could be seen. From then on, the described framework took control of the vehicle to drive it autonomously over the chain. We start by analysing the link detection performance. As the vehicle was moving at a low speed, many of the links were in the sonar's field of view enough time to be detected in multiple occasions. On the course of traversing the chain the detector produced a total of 376 detections, effectively detecting 10 different chain links. In order to evaluate the accuracy of the link detector independently of potential errors introduced in the two subsequent modules, we have manually labelled the link center on those images where a link was detected. Table I summarizes the number of times that each of the 13 links

were detected together with the mean error computed with respect to the labelled center.

Note that the first 3 links were never detected. This is due to the limited space in the test tank that did not allow for the necessary distance between the vehicle's starting position and the first chain links to be detected. The rest of the links were detected multiple times, depending on how much time they were in the sonar's field of view and how well they were observed. Regarding the accuracy, all link centers have an estimated error below 15 cm. These errors are due to the variability of the template matching step as well as the assumption of the 2D projection when determining the link centers. Relatively to the link size, they are all below 1/4 of the link's length and therefore we can consider that we achieve acceptable detection accuracy.

TABLE I: Table showing the number and accuracy (compared to manually labelled link centers) of the link detections along the chain following experiment.

Link Num.	Link Detections	Mean Error (cm)	Link Num.	Link Detections	Mean Error(cm)
1	0	-	8	33	4.5 ± 3.9
2	0	-	9	83	7.9 ± 9.5
3	0	-	10	23	6.8 ± 14.1
4	22	12.3 ± 3.6	11	30	10.2 ± 13.3
5	12	6.5 ± 9.2	12	21	9.9 ± 5.9
6	5	7.2 ± 5.1	13	122	5.6 ± 16.3
7	25	4.8 ± 4.7			

Figure 5 shows the link detections plotted on the world frame (in green), together with the waypoints (in red) that the planner module has associated to the detections and the AUV trajectory (in blue). It is important to remark that the link waypoints are dynamically recomputed during all the experiment as new detections appear by following the procedure described in Section IV. In this sense, the depicted link waypoints are the last estimation for each link. These online adjustments in the position of the waypoints together with the small vehicle displacements induced on the turn around movements explain the slightly jagged trajectory of the AUV. Since the test chain was short, when the vehicle reached the middle of the chain the farthest links were no longer visible, thus triggering the turn around movement at each waypoint. It is also worth noting that a distance threshold of 0.03 meters was used to consider whether the vehicle had arrived to a waypoint. For this reason, the AUV trajectory does not go over the exact position of the link waypoints but effectively passes through the tolerance areas shown with red dashed circles.

Regarding the performance of the planner module, we observe, in the first place, that the links have been correctly associated to the scattered detections. Moreover, the vehicle is driven successfully through the sequence of waypoints. To verify that the performed trajectory went over the actual chain links we require the absolute positions of each link. Unfortunately this ground truth is not available. As an alternative we can compare the estimated link waypoints of the trajectory against a visual mosaic of the acquired images along the experiment. The mosaic is referenced with

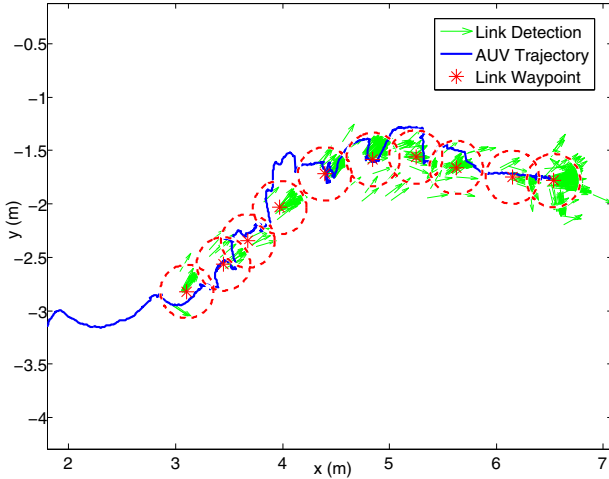


Fig. 5: AUV trajectory along the chain following experiment (in blue). Green arrows represent the center and orientation of the multiple link detections. In red, the estimation of the link waypoints provided by the planner with a circle depicting the tolerance region at 0.03 meters.

respect to the first sonar frame and therefore can also be referenced in world coordinates by using the vehicle location where the first frame was gathered. To build such a mosaic we have computed the pairwise registration of each frame with a window of frames in its neighborhood using Fourier-based techniques [8]. All the obtained pose constraints have been used in a pose-based graph optimization, that lead to the maximum likelihood configuration of the sonar images. Finally the frames can be fused by simply averaging the pixel intensities at each location. Figure 6 shows the link waypoints overlaid on the acoustic mosaic. The obtained mosaic is, in general, visually consistent. However, the raw images were affected by several reflections and intensity artefacts causing a lack of definition in some mosaic areas. As it can be seen, the computed link waypoints closely follow the chain link centers thus testifying the accuracy of our chain following scheme. The last waypoints present small deviations, possibly due to the fact that the vehicle accumulated drift along the trajectory. To address that, in future work we could deploy absolute localization beacons or integrate the framework within a simultaneous localization and mapping approach in order to bound the navigation drift.

VII. CONCLUSIONS AND FUTURE WORK

We have presented an approach that brings together image processing, planning and control algorithms to autonomously follow a chain. To the best of the author's knowledge this is the first attempt on autonomous chain tracking underwater. The use of a FLS has motivated the development of new algorithms to tackle the problem in a robust way, thus dealing with the noise, the intensity artefacts and the sonar's narrow field of view. Results have shown that the developed detection algorithm can accurately identify the position of the chain links in the acoustic images. Moreover, the planning

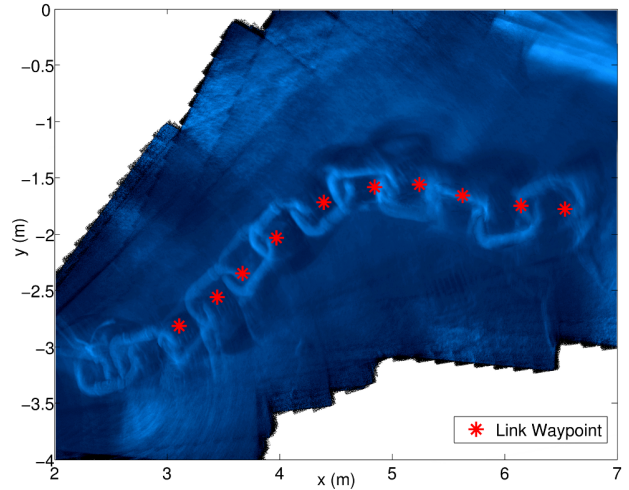


Fig. 6: Acoustic mosaic generated by registering the acquired sonar frames along the vehicle trajectory with the link waypoints overlayed in red. The link waypoints closely follow the actual link locations.

approach is able to correctly associate the multiple detections with the corresponding link waypoints and the control system keeps track of the links in view while driving the vehicle along the chain. The visual consistency of the visited waypoints on a mosaic generated by registering the acquired frames, proves that the vehicle has performed a trajectory closely following the link's centers.

Future work will involve the integration of the water jet and a new low-level controller [6] to perform chain following while compensating accordingly for the force/torque disturbances produced by the jet. Besides, the chain following capability will be tested at sea where we expect a better performance as the sonar images will not be affected by the reflections and multi-paths typical of the water tank scenario.

REFERENCES

- [1] "PANDORA: Persistent autonomy through learning adaptation and re-planning," 2014, retrieved June , 2014, from <http://www.persistentautonomy.com>.
- [2] A. Hall, "Cost effective mooring integrity management," in *Offshore Technology Conference*, 2005.
- [3] C. Morandini and F. Legersteet, "Consistent integrity of mooring systems," *ISOPE, Osaka, Japan*, 2009.
- [4] Noble Denton Europe Limited, "Research report 444 floating production system," Health and Safety Executive (HSE), Tech. Rep., 2006.
- [5] "Aris explorer 3000," 2014, retrieved June 2014, from <http://www.soundmetrics.com/Products/ARIS-Sonars/>.
- [6] G. Karras, C. Bechlioulis, S. Nagappa, N. Palomeras, K. Kyriakopoulos, and M. Carreras, "Motion control for autonomous underwater vehicles: A robust model - free approach," in *Proceedings of the Int. Conf. on Robotics and Automation ICRA'14*, 2014.
- [7] N. Hurtos, S. Nagappa, X. Cufí, Y. Petillot, and J. Salvi, "Evaluation of registration methods on two-dimensional forward-looking sonar imagery," in *OCEANS'13 MTS/IEEE*, 2013.
- [8] N. Hurtos, X. Cufí, Y. Petillot, and J. Salvi, "Fourier-based registrations for two-dimensional forward-looking sonar image mosaicing," in *IEEE/RSJ Int. Conf. on Intelligent Robots and Systems (IROS)*, oct. 2012, pp. 5298 –5305.
- [9] D. Ribas Romagós, N. Palomeras Rovira, P. Ridao Rodríguez, M. Carreras Pérez, and A. Mallios, "Girona 500 AUV: From survey to intervention," *IEEE/ASME Transactions on Mechatronics*, 2012, vol. 17, núm. 1, p. 46-53, 2012.